Multi-analytical study of historical semiconductor pigments

V. Capogrosso

*Politecnico di Milano, Dipartimento di Fisica - Piazza Leonardo da Vinci, 32
20133 Milano, Italy*

Summary. — This work is focused on the study of semiconductor-based pigments, which substituted traditional pigments in the second half of the 19th century. Synthetic semiconductor pigments may be chemically unstable due to the presence of many impurities unintentionally introduced during manufacturing. The aim of this work is to provide an insight on the application of X-ray Fluorescence (XRF) for the analysis of these painting materials, including both Cd- and Zn-based pigments. Three different approaches have been followed: the semi-quantitative analysis of samples with similar elemental composition, the complementary use of XRF and Raman spectroscopy for the analysis of elemental and molecular composition and the synchrotron-based XRF and XANES for the detection of impurities. The synergetic combination of different techniques provides information useful for the definition of specific markers for future analysis of paint-samples with implications for the conservation and treatment of late 19th and early 20th century paintings.

PACS 78.70.En – X-ray emission spectra and fluorescence.
PACS 81.70.Jb – Chemical composition analysis, chemical depth and dopant profiling.
PACS 82.80.Gk – Analytical methods involving vibrational spectroscopy.
PACS 82.80.Ej – X-ray, Mossbauer, and other γ-ray spectroscopic analysis methods.

1. – Introduction

A range of semiconductor pigments was introduced in the second half of 19th century and substituted the pigments used by painters in earlier times. This new class of synthetic pigments was based on Zn and Cd calcogenides. Recent studies, focused on the analysis of both modern paintings and historical and model samples containing Zn and Cd pigments, have highlighted the presence of impurities, changes in manufacturing processes as well as different degradation paths [1]. *In situ* luminescence imaging and spectroscopy of a painting by Van Gogh has highlighted a peculiar luminescence emission attributed to copper impurities in a zinc-based white pigment [2]. In parallel, spectroscopic investigations on both pure ZnO and paint models have demonstrated that physical and

chemical interactions affect the UV and visible emissions, leading to the observation of considerably different emission profiles [3]. Others have employed luminescence of Cd-based pigments which emit in the infrared to discriminate among different mixtures in paintings [4]. While luminescence allows mapping of the distribution of similar signal, elemental information from pigments is commonly used for their identification. Portable X-ray fluorescence (XRF) spectroscopy, which operates with a spatial resolution of few mm, has been extensively used for the analysis of pigments. XRF is a non-destructive, multi-elemental, fast and cost-effective analytical technique and it is one of the methods most often applied for obtaining qualitative and semi-quantitative information on materials under study [5]. One of the main advantages of XRF is that, not requiring vacuum, it can be applied in air directly on a sample without any preparation. This feature makes XRF spectrometry very suited for the analysis of cultural heritage objects that are unique and often cannot be moved [6]. Over the last decade advances in X-ray generation and detection have led to the evolution of instrumentation from laboratory-based standalone units to highly portable and lightweight handheld devices [7]. XRF can be used to recover the chemical elemental composition of the sample under study with a high sensitivity, but in most of the cases cannot give the exact identification of the pigment. For example in the case of green pigments such as malachite ($2CuCO_3Cu(OH)_2$), used primarily by Egyptians, and verdigris ($Cu(OH)_2$ ($CH_3COO)_25H_2O$), introduced by Greeks, they both contain Cu, but the first is a basic copper (II) carbonate and the last is a basic copper acetate. All ochre pigments are natural and contain iron oxide (III) (Fe_2O_3) as their main component. The identification is rather complicated and implies the identification of the characteristic iron oxide or hydroxide material. The combination of XRF with complementary molecular spectroscopy is thus required for pigment identification, which can be achieved by Raman spectroscopy or X-ray Diffraction [8]. In particular, the interpretation of elemental data, like that acquired with XRF is complemented and corroborated by the molecular characterization of samples with Raman spectroscopy, which provides information regarding the molecular structure of the material under investigation. In the last decades the applicability of XRF has been extended with the dawn of synchrotron-radiation based μ-XRF at particle accelerators giving access to submicron resolution and superior sensitivity with respect to conventional *in situ* XRF. In fact, the high-energy synchrotron X-ray beam provides sensitivities three orders of magnitude higher than Scanning Electron Microscopy coupled to Energy Dispersive X-ray spectroscopy (SEM-EDX), leading to sub-ppm sensitivity. The use of XRF for art and archaeology, conducted using μ-XRF instruments installed at synchrotron beamlines and with laboratory and transportable equipment, known as portable-XRF (or PXRF), was reviewed in 2000 by Janssens *et al.* [9], underlining the main interests of synchrotron-based XRF in the context of the study of a wide variety of materials of cultural heritage. Furthermore, μ-XRF in combination with μ-X-ray Absorption Near Edge Spectroscopy (XANES) is a powerful analytical method for probing the spatial distribution and valence of a given chemical element on the microscopic scale [10,11]. High resolution XRF mapping was described by Casadio as a probe to obtain highly spatially resolved and sensitive maps of metal impurities in submicron particles of ZnO pigments [12]. The last frontier of XRF spectroscopy is the knowledge of the stratigraphy of a painting thanks to the high penetration depth of X-rays. Just some micrometers below a painting surface a great amount of information can be present in the form of underdrawings, underpaintings and alterations. For instance, macroscopic scanning XRF (MA-XRF) has been employed to visualize the distribution of specific pigments within some of these layers [13]. This work illustrates the study of commercial Cd- and historical Zn-based painting samples

probing the effectiveness of XRF spectroscopy alone or in combination with other techniques. First qualitative and a semi-quantitative XRF analysis on commercial Cd-based pigments is proposed in order to determine the concentration of calcogenides relative to Cd, and to discriminate similar yellow pigments on the basis of their elemental composition. On a sample of a 20th century historical red pastel conventional XRF is applied in combination with Raman spectroscopy for getting clear markers of its composition. Synchrotron radiation is finally used to investigate micrometric trace impurities in samples; an example of this approach for the analysis of a white Zn-based historical pigment is presented in the last section, where microscopic heterogeneities are investigated by means of μ-XRF mapping and μ-XANES.

2. – Methods

2'1. *Laboratory portable XRF spectroscopy*. – XRF measurements were carried out using a portable XRF spectrometer (Elio, XGLab srl). The instrument is a fast system with large area Silicon Drift Detector (SDD) ($25\,mm^2$) and it is particularly efficient due to the X-ray generator that can reach up to $50\,kV$ and to a high solid detection angle geometry. Excitation source works with a Rh anode and the beam is collimated to a spot diameter on the sample surface of about $1.3\,mm$. XRF data has been processed using the PyMca software, which has also been used to obtain fluorescence maps [14]. Single element imaging has been performed setting Regions Of Interest (ROI) around the characteristic element peaks.

2'2. *Raman spectroscopy*. – Raman measurements, in back-scattering configuration, have been performed using a laboratory spectrometer coupled with a cooled CCD camera [15]. Excitation, provided by a $785\,nm$ diode laser source, is coupled to an optical fiber connected to a micro-probe, which allows the micrometric analysis of a single point of interest with a spatial resolution of about $100\,\mu m$ at a working distance of $3\,mm$.

2'3. *Synchrotron-based μ-XRF and μ-XANES spectroscopies*. – μ-XRF mapping and μ-XANES measurements have been carried out at the LUCIA beamline at SOLEIL synchrotron radiation facility [16]. The LUCIA beamline is a tender (0.8–8 keV) X-ray microprobe able to detect chemical speciation and to carry out elemental mapping by μ-XANES and μ-XRF spectroscopy respectively. The instrument uses a photon source based on an undulator of the APPLE-II type and a double crystal monochromator for selecting X-ray energy. Experiments were performed in low a vacuum chamber in which samples were placed on a micro positioning (x, y, z) sample stage. Fluorescence spectra have been collected using a 4-element SDD detector. μ-XRF maps of $100 \times 100\,\mu m^2$ with step of $3\,\mu m$ have been collected using a beam spot size of $3 \times 3\,\mu m^2$ with an excitation energy of $7.4\,keV$ for the analysis of different elements. At this energy only X-ray fluorescence L-lines of Zn at $1.0\,KeV$ are excited and detected. μ-XANES spectra have been acquired simultaneously measuring the fluorescence yield (FY) and the total electron yield (TEY). XANES spectra have been collected at Cr K-edge.

3. – Materials

Cd-based pigments were purchased from Kremer Pigmente GmbH & Co (Germany) as finely pigment powder. The pigments selected can be considered as binary alloys of ZnS and CdS and of CdS and CdSe obtained through a high substitution ratio of Cd

TABLE I. – *Cadmium pigments: colour, chemical composition and relative amount of Cd, Zn, S and Se normalized to the maximum signal of the dataset.*

Sample	Colour	Chemical composition	Cd	Zn	S	Se
KP1	Yellow lemon	Cd(Zn,S)	0.8	1	1	0
KP2	Yellow light	Cd(Zn,S)	0.85	0.36	0.77	0
KP3	Yellow medium dark	Cd(Zn,S)	1	0.07	0.76	0
KP4	Yellow dark	Cd(Zn,S)	0.86	0.05	0.76	0.02
KP5	Orange very light	Cd(S,Se)	0.84	0.03	0.79	0.52
KP6	Orange light	Cd(S,Se)	0.83	0.03	0.63	0.67
KP7	Red light	Cd(S,Se)	0.58	0.02	0.29	0.81
KP8	Red purple	Cd(S,Se)	0.57	0.02	0.2	1

to Zn and of S to Se. Eight different shades were chosen for the present study, ranging from light yellow to deep red. Paint samples were prepared using Plextol D498 as the binding medium and by applying a thin paint layer on quartz supports. The two Zn-based samples analyzed are representative of different artist materials available at the turn of the 20th century: a pastel and a pigment from which they were made. The small red fragment pastel belongs to a collection of Raffaelli pastels by Lefranc-Bourgeois, which at the beginning of the 20th century was the largest producer of ZnO in Europe. The second sample is a paint tube of Chinese white Winsor & Newton from the Courtauld Institute of Art, London.

4. – Results

$4^.$1. *Semi-quantitative XRF.* – Semi-quantitative XRF allows a rough estimation of the elemental composition. This method does not provide absolute concentration values, but it can be used to determine the relative elemental concentrations in different samples. The approach was performed on the commercial Cd-based painting materials in order to verify the chemical composition of different hues of Cd-based yellows and reds [17]. In fact, the colour of Cd-based sulphides can be modified with the addition of Zn to obtain a lighter colour; in contrast, to obtain a deeper red colour, Se atoms replace S atoms in the hexagonal CdS lattice. These replacements are reflected in modifications in the band gap characteristic of the semiconductor pigments [18]. The list of the material with their chemical composition is reported in table I.

For semi-quantitative analysis, the same amount of material was irradiated for the same time $(60\,\text{s})$, with the same geometric conditions. The experimental settings of the X-ray tube were fixed at a voltage of $40\,\text{KV}$ and a current of $40\,\mu\text{A}$. In fig. 1 representative XRF spectra of a yellow, orange and red sample are reported.

Relative amounts of the elements detected (Cd, Zn, S and Se) amongst samples have been calculated by normalizing the counts of the maximum signal at the $K\alpha$ line of the dataset (see table I). The composition varies from a high concentration of Zn in the lighter yellow shadows to an increase in the concentration of cadmium in the dark yellow and Se in the red hues—slight differences in the spectra confirm the relative sensitivity of XRF to small variations in concentration of chemical elements. In order to carry out quantitative analysis of the samples, precise calibration and standard samples
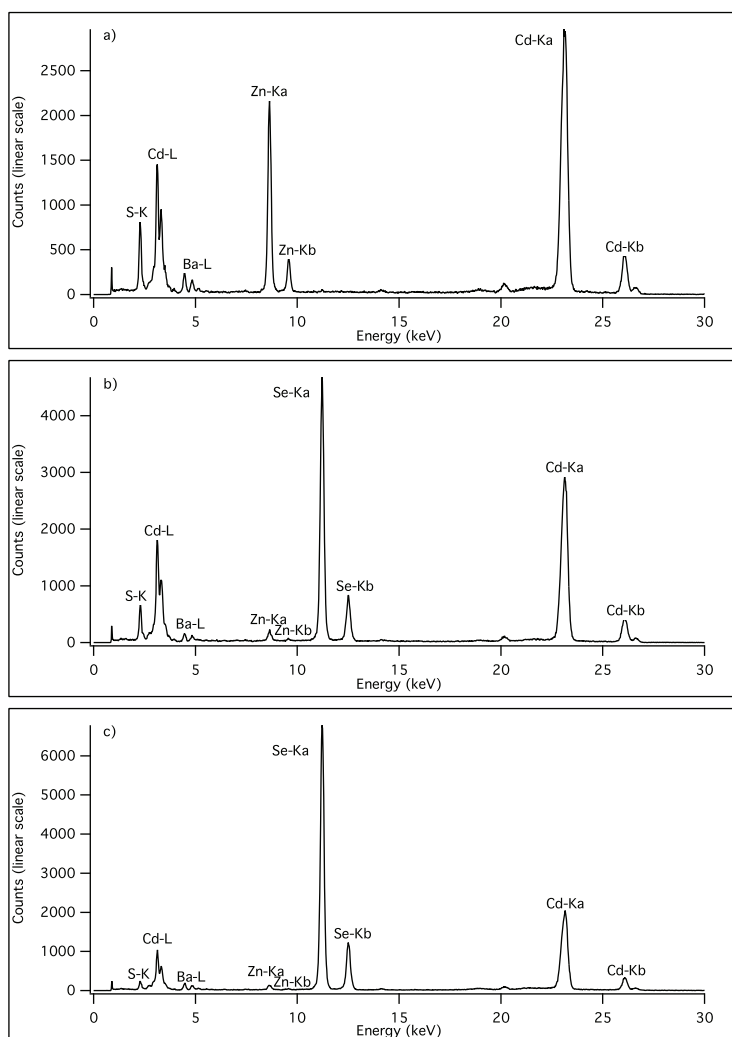
Fig. 1. – a) XRF spectrum of KP2 sample (yellow); b) XRF spectrum of KP6 sample (orange); c) XRF spectrum of KP8 sample (red).

would be required to relate specific known concentrations to peak heights. For accurate quantitative analysis the thickness of the sample must be enough to attenuate all primary X-rays from the XRF instrument.

4˙2. *XRF combined with Raman spectroscopy*. – In order to demonstrate the effectiveness of the combination between XRF and Raman spectroscopy for the study of pigments, the red Lefranc pastel fragment was analyzed. The XRF spectrum, as reported in fig. 2, is dominated by an overall composition of Zn along with minor quantities of Fe and traces of Ba, Co and Ni.

Raman spectroscopy confirms the presence of ZnO; additional bands at 224, 291, 407, 495 and 610 cm^{-1} indicate the presence of a synthetic iron oxide pigment, *Mars Red*
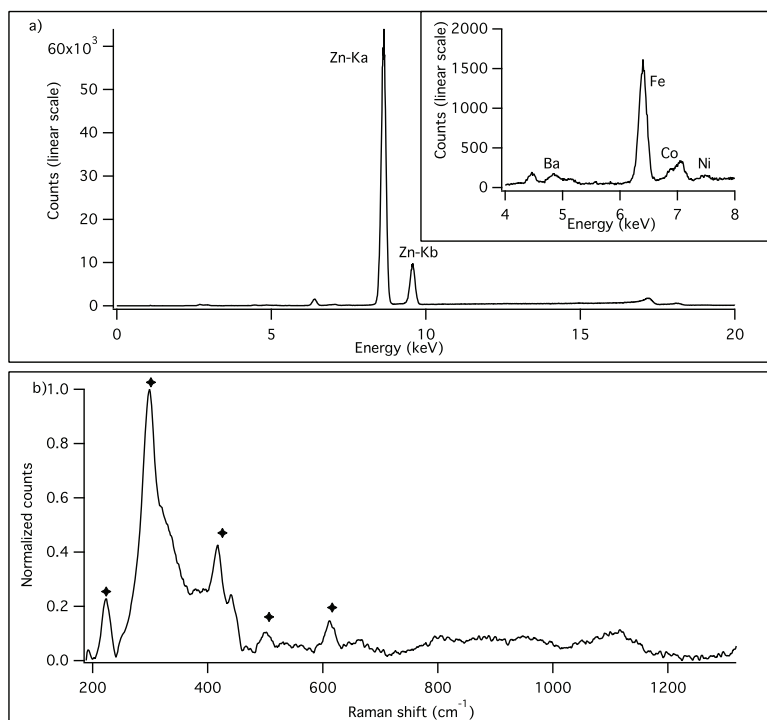
Fig. 2. – a) XRF spectrum of red Lefranc pastel (in the inset the zoom of the energy area between 4 and 8 keV); b) Raman spectrum of red Lefranc pastel. The markers identify the Raman bands at 224, 291, 407, 495 and 610 cm^{-1}.
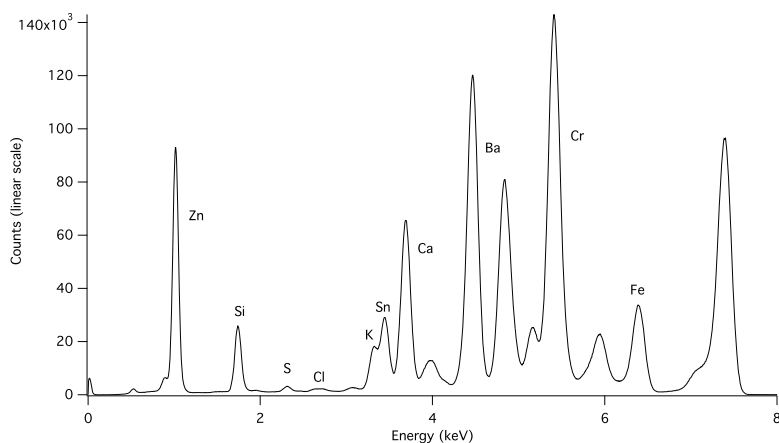

Fig. 3. – μ-XRF cumulated spectrum of the Winsor and Newton sample, obtained as the sum in all points of a mapped area of $100 \times 100\,\mu\text{m}^2$.

(Fe_2O_3). This pigment was first made in the laboratory during the 18th century and from the 19th century the manufacturing started on a regular basis and it was found to have all the properties, including durability and permanence, of its natural counterpart, *Red Ochre*.
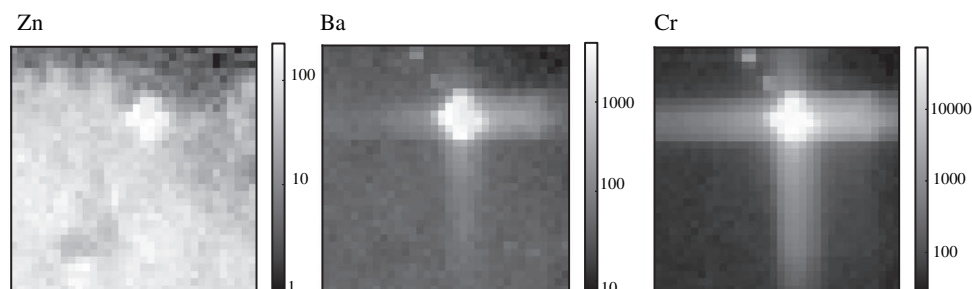
Fig. 4. – μ-XRF maps showing the spatial distribution of Zn, Ba and Cr over an area of $100 \times 100\,\mu m^2$ with a step of $3\,\mu m$. The maps are reported in logarithmic scale.
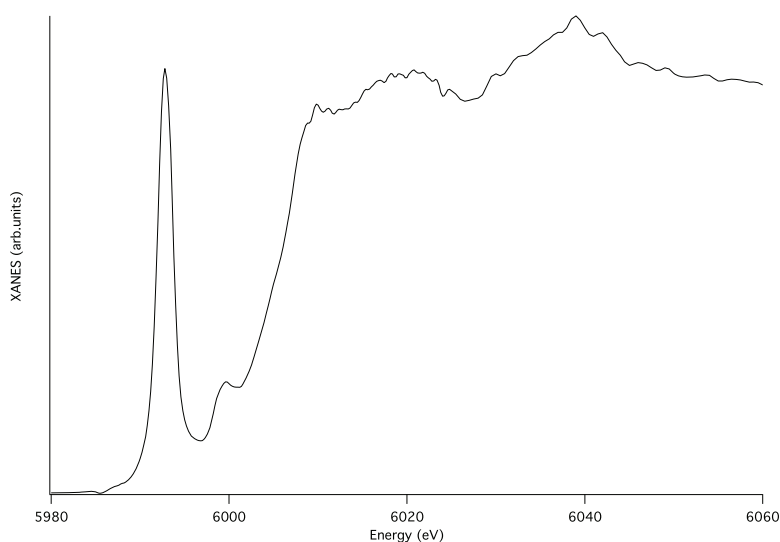

Fig. 5. – μ-XANES spectrum at Cr K-edge performed in the same area of the Cr heterogeneity highlighted in the Cr map (see fig. 4).

4˙3. *μ-XRF synchrotron mapping combined with μ-XANES*. – After preliminary elemental and molecular characterization using XRF and Raman spectroscopies (that are not reported in this work), the presence of trace metal ions in the Zn-based Winsor & Newton paint tube has been investigated with synchrotron radiation, which has the advantage of being tunable and coupled with microscopic resolution [19].

In fig. 3 the cumulative spectrum from μ-XRF mapping, fitted using Pymca, is reported. Beside Zn, the analysis highlights the presence of significant amounts of Ba and Cr, combined with traces of Ca, Fe and Si. Weak signals assigned to K, S, and Cl are also observed. The mapping capabilities of the approach shows the excellent spatial correlation between Ba, Cr and Cl distributions in an agglomerate of $20\,\mu m$ in diameter (see fig. 4). In order to clarify the chemical nature of the agglomerate, μ-XANES measurements have been performed on the same area for inspecting the oxidation state of the Cr point. The measured chromium K-edge μ-XANES spectrum (reported in fig. 5) shows a well-defined pre-edge peak at $5.993\,keV$, typical of Cr(VI) compounds having a

tetrahedral coordination geometry. The spectrum is comparable with the one of $BaCrO_4$ reported by Monico [20], which suggests the presence of barium chromate as an unintentional contamination introduced during the mixing of the pigments in the white paint.

5. – Conclusions

This work proposes conventional and synchrotron XRF spectroscopy as a versatile tool to be used alone or combined in a synergetic manner with other analytical techniques for investigating commercial and historical semiconductor-based pigments. The knowledge of the relative amount of different constituents of a paint is crucial for a careful program of conservation of polychrome works. Moreover, the combination between XRF and Raman techniques is a well-established method for the identification and chemical characterization of pigments. In the case of impurities in pigments, synchrotron-based analysis with a micrometric resolution is really powerful for investigating heterogeneous impurities where both μ-XRF and μ-XANES can yield important information. The proposed approach, based on the fitting of XRF data, the application of non-destructive and complementary molecular spectroscopy and the analysis of micro-samples with tunable X-ray sources, can be extended to the analysis of more complex and heterogeneous samples, but data always require careful interpretation. Data obtained using the techniques described in this work can inform the definition of elemental markers for future *in situ* analysis of paint-samples with implications for the analysis of semiconductor-based pigments from the early 20th century paintings.

<center>* * *</center>

REFERENCES

[1] Mass J., Sedlmair J., Patterson C. S., Carson D., Buckley B. and Hirschmugl C., *Appl. Phys. A*, **106** (2011) 25.
[2] Comelli D., Nevin A., Brambilla A., Osticioli I., Valentini G., Toniolo L., Fratelli M. and Cubeddu R., *Appl. Phys. A*, **106** (2011) 25.
[3] Clementi C., Rosi F., Romani A., Vivani R., Brunetti B. G. and Miliani C., *Appl. Spectr.*, **66** (2012) 1233.
[4] Delaney J. K., Zeibel J. G., Thoury M., Littleton R., Palmer M., Morales K. M., Rene de la Rie E. and Hoenigswald A., *Appl. Spectr.*, **64** (2010) 584.
[5] Mantler M. and Schreiner M., *X-Ray Spectrom.*, **29** (2000) 3.

[6] SHUGAR A. N. and MASS J. L., *Handheld XRF for Art and Archaeology* (Leuven University Press) 2012.

[7] HOCQUET F., GARNIR H., MARCHAL A., CLAR M., OGER C. and STRIVAY D., *X-Ray Spectrom.*, **37** (2008) 304.

[8] RAMOS P. M., RUISANCHEZ I. and ANDRIKOPOULOS K. S., *Talanta*, **75** (2008) 92636.

[9] JANSSENS K., VITTIGLIO G., DERAEDT I., AERTS A., VEKEMANS B., VINCZE L., WEI F., DERYCK I., SCHALM O., ADAMS F., RINDBY A., KN A., SIMIONOVICI A. and SNIGIREV A., *X-Ray Spectrom.*, **29** (2000) 7391.

[10] BERTRAND L., ROBINET L., THOURY M., JANSSENS K., COHEN S. X. and SCHDER S., *Appl. Phys. A*, **106** (2011) 377396.

[11] COTTE M., SUSINI J., DIK J. and JANSSENS K., *Acc. Chem. Res.*, **43** (2010) 705714.

[12] CASADIO F. and ROSE V., *Appl. Phys. A*, **111** (2013) 18.

[13] JANSSENS K., DIK J., COTTE M. and SUSINI J., *Acc. Chem. Res.*, **43** (2010) 814825.

[14] SOLE V. A., PAPILLON E., COTTE M., WALTER P. and SUSINI J., *Spectrochim. Acta Part B At. Spectrosc.*, **62** (2007) 6368.

[15] BRAMBILLA A., OSTICIOLI I., NEVIN A., WALTER P. and SUSINI J., *Spectrochim. Acta Part B At. Spectrosc.*, **62** (2007) 6368.

[16] FLANK A.-M., CAUCHON G., LAGARDE P., BAC S., JANOUSCH M., WETTER R., DUBUISSON J.-M., IDIR M., LANGLOIS, MORENO T. and VANTELON D., *Nucl. Instrum. Methods Phys. Res. B Beam Interact. Mater. At.*, **246** (2006) 269274.

[17] CESARATTO A., D'ANDREA C., NEVIN A., VALENTINI G., TASSONE F., ALBERTI R., FRIZZI T. and COMELLI D., *Anal. Methods*, **6** (2014) 130.

[18] ANGLOS D., SOLOMIDOU M., ZERGIOTI I., ZAFIROPULOS V., PAPAZOGLOU T. and FOTAKIS C., *Appl. Spectrosc.*, **50** (1996) 1331–1334.

[19] CAPOGROSSO V., GABRIELI F., BELLEI S., CARTECHINI L., CESARATTO A., TRCERA N., ROSI F., VALENTINI G., COMELLI D. and NEVIN A., *J. Anal. At. Spectrom.*, **30** (2015) 828 DOI: 10.1039/C4JA00385C.

[20] MONICO L., VAN DER SNICKT G., JANSSENS K., DE NOLF W., MILIANI C., VERBEECK J., TIAN H., TAN H., DIK J., RADEPONT M. and COTTE M., *Anal. Chem.*, **83** (2011) 12142.